

## Reconstruction of Steps on the Si(111) $2 \times 1$ Surface

R. M. Feenstra and Joseph A. Stroscio

IBM Thomas J. Watson Research Center, Yorktown Heights, New York 10598

(Received 10 August 1987)

The structure of steps on cleaved silicon (111) surfaces is studied by scanning tunneling microscopy. Predominantly  $[2\bar{1}\bar{1}]$ -oriented steps are observed. Ordered regions of individual steps have unit periodicity along the step edge. A  $\pi$ -bonded reconstruction of the step edge is deduced from the images.

PACS numbers: 61.16.Di, 68.35.Bs

There are several reasons for studying the geometric and electronic structure of steps on cleaved silicon (111) surfaces. First, deduction of the structure of the steps is intrinsically interesting. Second, an understanding of step structure leads naturally to possible insights into the structure of higher-index faces such as (112) or (113) surfaces, which are themselves a periodic array of low-index steps.<sup>1</sup> Third, the epitaxial growth of other semiconductors (GaAs or GaP) on silicon appears to depend on the step structure of the surface.<sup>2,3</sup> Finally, this study of steps illustrates the utility of scanning-tunneling-microscope (STM) images for the analysis of low-symmetry surface structure.

In this work we present STM images obtained from cleaved Si(111) surfaces. The structure of  $2 \times 1$ -reconstructed terraces has been studied in previous work<sup>4</sup>; here, we focus on the structure of steps on the surface. We observe predominantly  $[2\bar{1}\bar{1}]$ -oriented steps, in agreement with previous low-energy electron-diffraction studies.<sup>5</sup> When the  $2 \times 1$  reconstruction is oriented parallel to the step, two different periodic atomic arrangements are observed along the step edge. By comparing voltage-dependent STM images with various models for the steps, we identify the class of step reconstructions which occur. One observed arrangement is identified, for the first time, as a  $\pi$ -bonded reconstruction of the step edge.

The STM used in this work is similar to that described by Binnig and Rohrer,<sup>6</sup> and is described in detail elsewhere.<sup>4</sup> The microscope is contained in an ultrahigh-vacuum chamber with base pressure of  $< 4 \times 10^{-11}$  Torr. Silicon samples, *n*-type with resistivity of 0.01  $\Omega$  cm, were cleaved *in situ* along the  $[2\bar{1}\bar{1}]$  or  $[\bar{2}11]$  directions. Tungsten probe tips, prepared by electrochemical etching, were cleaned *in situ* by electron bombardment. The sharpness of the tips varied, as evidenced by varying widths of the observed steps. For all of the images analyzed here, the step edges are maximally sharp, with widths of  $1\frac{1}{3}$  double unit cells (8.9  $\text{\AA}$ ). Furthermore, in some portions of each image, we observe only a single topographic maxima per unit cell along the step edge, thus indicating that the probe tips are not introducing any spurious features in the images. All images are obtained at a constant tunneling current of 1 nA, and at

voltages specified below. All images (with the exception of those in Fig. 1) have been corrected for microscope drift in order to achieve the correct  $2 \times 1$  unit cell size of  $6.65 \times 3.84 \text{ \AA}^2$ . Simultaneous acquisition of images at multiple voltages was accomplished by a method described previously.<sup>4</sup> Structural models considered here are formed by truncation of the perfect diamond lattice or by truncation of a model of nonbuckled  $\pi$ -bonded chains. The coordinates of atoms in the immediate vicinity of the step are determined by a Keating-type strain-energy minimization.<sup>7</sup>

Figure 1 shows various images of steps on the

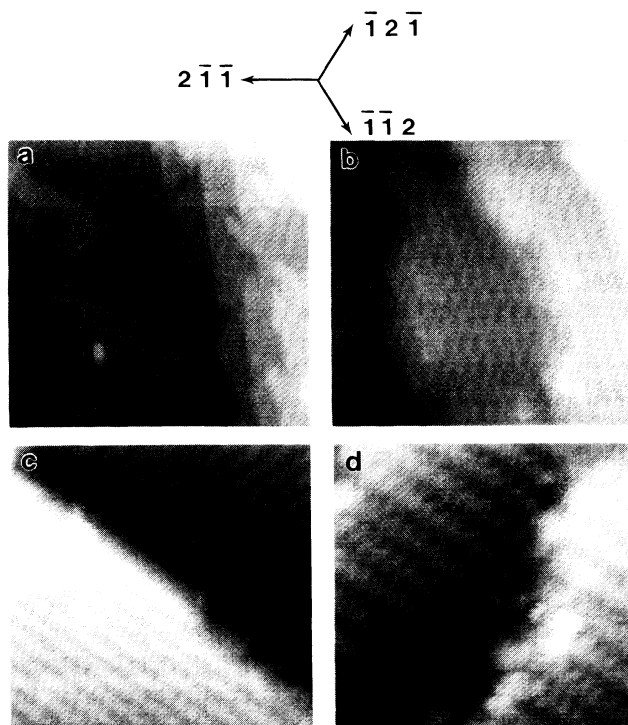


FIG. 1. Large-scale STM images of silicon (111) surfaces, showing atomic steps and the  $2 \times 1$  reconstruction. The images extend over lateral areas of (a)  $600 \times 600 \text{ \AA}^2$ ; (b), (c)  $120 \times 120 \text{ \AA}^2$ ; and (d)  $60 \times 60 \text{ \AA}^2$ .

Si(111) $2\times 1$  surface. In Fig. 1(a) we display a relatively large region of the surface in which seven different terraces are clearly visible, separated by steps of height 3.14 Å. The outwards normal vectors of all of the steps observed in Fig. 1(a) are directed in one of the equivalent  $\langle 2\bar{1}\bar{1} \rangle$  surface directions, as indicated in the top part of the figure (small deviations occur from these directions due to thermal drift in the images). In Figs. 1(b)–1(d) we show somewhat expanded views of the surface in which the  $2\times 1$  reconstruction of the terraces is now visible. The reconstruction extends right up to, and through, the steps. All of the steps in these images are 3.14 Å in height, and they are mostly directed in a  $\langle 2\bar{1}\bar{1} \rangle$  direction. We see that the  $2\times 1$  reconstruction can have its  $[2\bar{1}\bar{1}]$  axis oriented either parallel, or rotated, relative to the step direction. In either case the step edge can be ordered [Fig. 1(c)] or disordered [Figs. 1(b) and 1(d)]. Overall, we find that the energetics of the  $2\times 1$  domain formation and the step formation are not strongly coupled.

The main topic of this paper is the geometric structure of ordered step edges. One such step is shown in Fig. 2. There we show a perspective view in part (a), a top view in (b), and a cross-sectional cut of the data in (c). The perspective view gives a three-dimensional representation of the surface, with the grey-scale shading determined by the *local height* of the surface relative to a smooth background (the background is determined simply by our performing a running average of the data over an area of  $3\times 3$  Å<sup>2</sup>). This type of shading is chosen to provide the best *qualitative* view of the surface. For *quantitative* measurement, we use cross-sectional cuts. In Fig. 2, two regions of the step edge are apparent in the upper and lower parts of the figure. Both regions have unit periodicity along the step edge ( $[01\bar{1}]$  direction). The lower region consists of a row of maxima in the images, with one maxima per unit cell. This row splits into two in the upper part of the image. The corrugation along these two rows is weak, but can be clearly seen in Fig. 2(a). A cross section through this upper region of the image is shown in Fig. 2(c). The two rows observed along the step edge give rise to maxima in the STM contour, with the rows separated laterally by  $4.5 \pm 0.5$  Å.

In the structural models discussed below for the step, we find two dangling bonds per unit cell along the step edge. This number is consistent with that observed in the upper part of Fig. 2. However, in the lower part of the figure we only observe one maximum per unit cell. This observation suggests that at the particular voltage used in Fig. 2, we may be imaging only one of the two dangling bonds (the connection between STM images and dangling bonds is discussed in more detail below). We therefore have performed a voltage-dependence study of the step images, shown in Fig. 3. In Fig. 3(a) we show a region of a step, imaged at 1.2 V, which is similar to that in Figs. 2(a) and 2(b). In Figs. 3(b) and

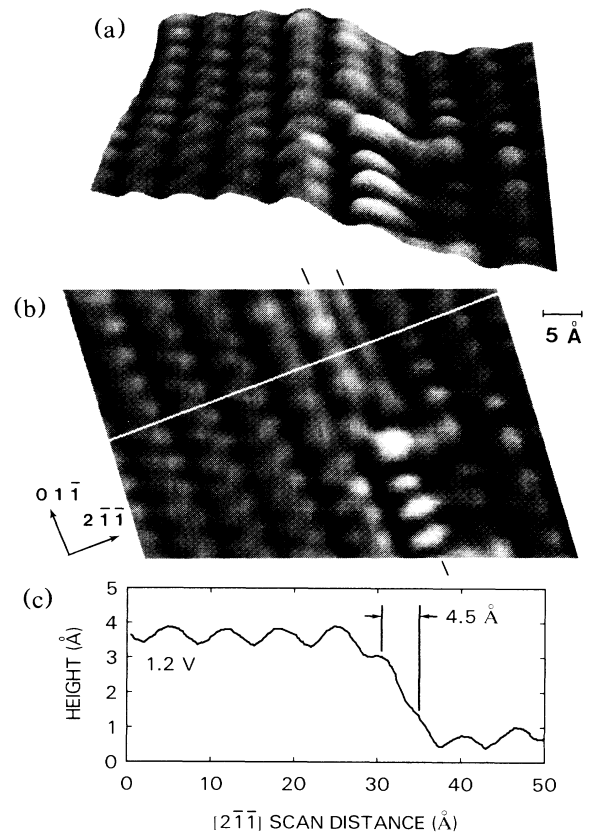


FIG. 2. STM image of a step on Si(111), acquired at sample voltage of +1.2 V; (a) perspective view, (b) top view of the same data, and (c) cross-sectional cut along the line indicated in (b). The step edge is identified by tic marks at the border of the image in (b).

3(c) we show the same region of the step, now imaged simultaneously at voltages of +1.5 and  $-1.5$  V. Tic marks on the images denote the step edge. We see that, along the step edge, the maxima in the images shift by half a unit cell ( $1.92$  Å) in the  $[01\bar{1}]$  direction from Fig. 3(b) to 3(c), thus demonstrating the existence of two dangling bonds per unit cell along the step edge. One dangling bond is seen at positive voltage, and the other at negative voltage. A similar reversal is observed on the ordered terraces at lower voltages,<sup>4</sup> although this effect on the terraces is suppressed at the voltages used in Fig. 3. Cross-sectional cuts through the images are shown in Fig. 3(d). We find that, at the step edge, the  $[2\bar{1}\bar{1}]$  shift of the maxima in the STA contour is small, about  $0.5 \pm 0.5$  Å. Note that this result does not depend on the position at which the cross-sectional cuts are taken; the dashed line in Fig. 3(d) was taken half a unit cell above the position indicated in Fig. 3(c), and the resulting shift is the same.

Our approach for determining geometric structure

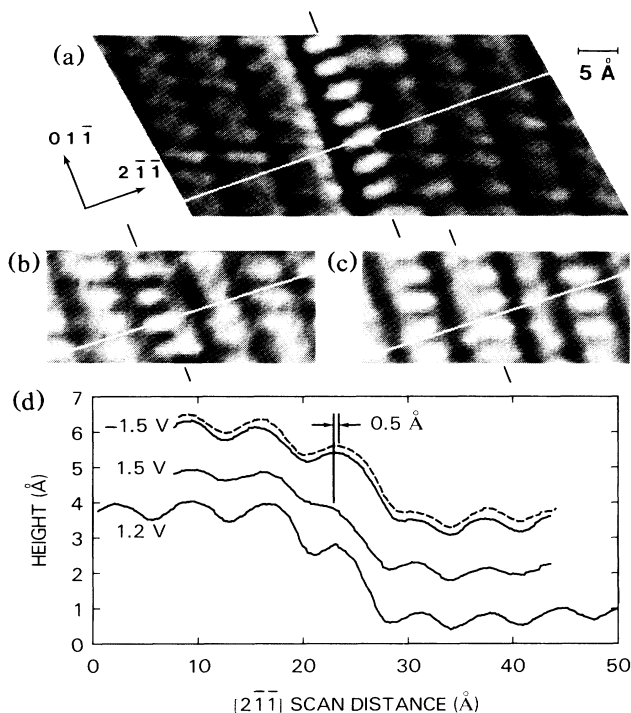


FIG. 3. STM images at various sample voltages; (a) +1.2 V, (b) +1.5 V, and (c) -1.5 V. Images in (b) and (c) were acquired simultaneously. The step edge is identified by tic marks at the border of the images. Cross-sectional cuts of the data are shown in (d); solid lines are cuts taken along the lines indicated in (a)–(c), and the dashed line is a cut taken half a unit cell above the line shown in (c).

from the observed STM images follows our previous studies of Si(111)2×1 and GaAs(110) surfaces.<sup>4,8</sup> There, we found a one-to-one correspondence between the maxima observed in STM images and the dangling bonds at the surface. The states constituting different dangling bonds, in general, lie at different energies and must therefore be imaged at different tip-sample voltages. The observed maxima are not located *exactly* above the atoms which have dangling bonds; shifts of up to about 0.5 Å can be inferred by a comparison of theory with experiment.<sup>8</sup> Here, for steps on the Si(111)2×1 surface, we again have a case with two dangling bonds per unit cell, and, as demonstrated above, we observe two maxima in the STM images. We associate these observed maxima with the dangling bonds. The lateral position of the atoms will again vary somewhat from the observed position of the maxima. We do not expect this effect to be much greater than the spatial extent of the dangling bond, which is 1.0–1.5 Å. This value thus sets an uncertainty limit on our determination of atomic positions from the STM images.

Our comparison of the observed data with structural models proceeds in two steps. First, we determine the

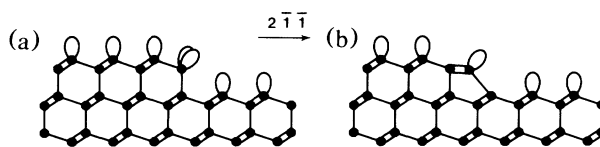


FIG. 4. Side view of two possible configurations for a  $[2\bar{1}\bar{1}]$  step.

class of possible structures. As shown above, all observed steps are of the  $[2\bar{1}\bar{1}]$  type (as opposed to  $[\bar{2}11]$ ). For this type, there are two possible classes,<sup>1,9</sup> shown in Fig. 4. The outermost atom at the step edge can either be twofold coordinated as shown in Fig. 4(a), or threefold coordinated as shown in Fig. 4(b). In Fig. 4(a), the dangling bonds form a “rabbit-ear” type arrangement, identical to that of the Si(100) surface. Then, we expect a dimerization along the step edge, leading to a double or quadruple periodicity along the edge, in contradiction to our observations. [Even without dimerization, the arrangement and number of dangling bonds pictured in Fig. 4(a) is completely inconsistent with our STM images.] In Fig. 4(b), the dangling bonds along the step edge form a stable structure with unit periodicity, in agreement with our observations. We therefore adopt this model as a starting point for the structure of the steps. We refer to this model as a “rebonded” configuration, since the edge atom rebonds to the lower terrace after cleavage.

We now add a  $\pi$ -bonded 2×1 reconstruction of the terraces to the model. To be consistent with experiment we consider a reconstruction which is parallel to the step edge, and in which the chains on the upper and lower terraces are separated by  $2\frac{1}{2}$  double unit cells (15.5 Å). Two models are then immediately possible, shown in Figs. 5(a) and 5(b). The models can be distinguished according to the topology of the ring structure of the upper terrace. The  $\pi$ -bonded reconstruction has ring structure 7575 . . . . The structure shown in Fig. 5(a) terminates the terrace with a fivefold ring. In Fig. 5(b), the step is terminated one single unit cell over, thereby adding a sixfold ring. Finally, in Fig. 5(c) we show a reconstruction of the model in Fig. 5(b), in which the fivefold and sixfold rings at the edge have interchanged to form nearest-neighbor dangling bonds at the step edge. We refer to this structure as a  $\pi$ -bonded reconstruction of the step. These three models for the step reconstruction are the only ones possible within the classes specified above.

Given the structural models shown in Fig. 5, and the STM images of Figs. 2 and 3, we are now in a position to compare the two. We focus on the  $[2\bar{1}\bar{1}]$  separation between dangling bonds at the step edge (in the orthogonal  $[0\bar{1}\bar{1}]$  direction in the models in Fig. 5 are consistent with both types of observed steps). In Fig. 5(a) the step-edge atoms with dangling bonds are third-nearest

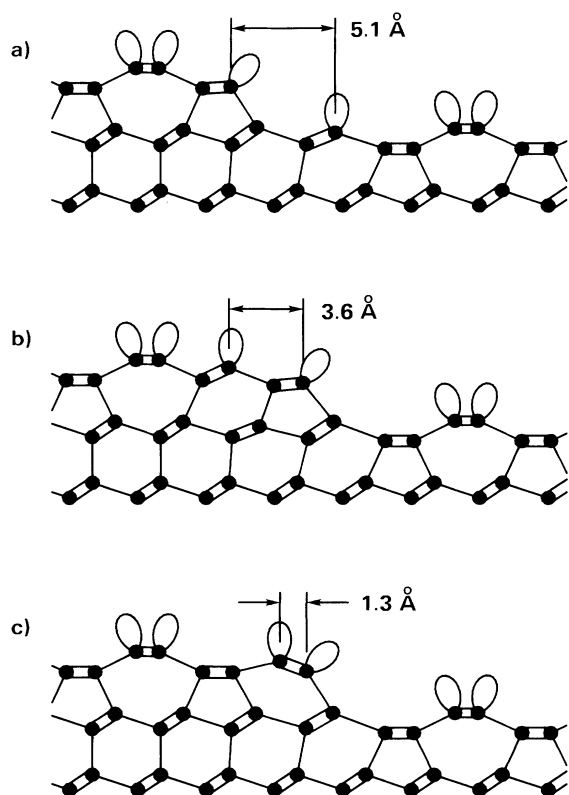


FIG. 5. Side view of models for the step reconstruction, including the  $2 \times 1$  reconstruction of the terraces.

neighbor, with a separation of about  $5.1 \text{ \AA}$ . In Fig. 5(b) these atoms are second-nearest neighbor with a separation of about  $3.6 \text{ \AA}$ , and in Fig. 5(c) the atoms are first-nearest neighbor with a separation of about  $1.3 \text{ \AA}$ . We compare these distances with the observed cross-sectional cuts. First, for Fig. 3(d) we found a separation of about  $0.5 \text{ \AA}$ . This value is consistent only with Fig. 5(c), even within the estimated uncertainty of  $1.5 \text{ \AA}$ . Thus we identify the structure observed in Fig. 3 (and the lower part of Fig. 2) as a  $\pi$ -bonded reconstruction of the step edge. Secondly, we consider the  $4.5\text{-\AA}$  separation observed in Fig. 2(c). This value falls in between

the values predicted in Figs. 5(a) and 5(b), and within our uncertainty range we cannot distinguish between these two models.

In summary, we have studied the structure of steps on cleaved Si(111) surfaces. We find that most observed steps are of the  $[2\bar{1}\bar{1}]$  type, with single periodicity along the step edge. Thus, we argue that the step edges are of the rebonded class, shown in Fig. 4(b). This result is consistent with previous arguments concerning the stability of such steps based on total-energy considerations,<sup>9</sup> and provides an explanation for the predominance of  $[2\bar{1}\bar{1}]$  steps compared to the  $[\bar{2}11]$  orientation.<sup>9</sup> Some regions of these steps are observed to reconstruct, forming nearest-neighbor dangling bonds along the step edge, that is, a  $\pi$ -bonded reconstruction of the step. This identification on the Si(111) $2 \times 1$  surface may lend some additional support to previous indications of related reconstructions on the Si(100),<sup>3</sup> Si(112),<sup>10</sup> and Si(113)<sup>11</sup> surfaces.

We gratefully acknowledge the technical assistance of A.P. Fein in this work.

<sup>1</sup>D. J. Chadi, Phys. Rev. B **29**, 785 (1984).

<sup>2</sup>S. L. Wright, M. Inada, and H. Kroemer, J. Vac. Sci. Technol. **21**, 534 (1982).

<sup>3</sup>D. E. Aspnes and J. Ihm, Phys. Rev. Lett. **57**, 3054 (1987), and references therein.

<sup>4</sup>J. A. Stroscio, R. M. Feenstra, and A. P. Fein, Phys. Rev. Lett. **57**, 2579 (1986), and J. Vac. Sci. Technol. A (to be published).

<sup>5</sup>M. Henzler, Surf. Sci. **36**, 109 (1973).

<sup>6</sup>G. Binnig and H. Rohrer, Helv. Phys. Acta **55**, 726 (1982), and Surf. Sci. **152/153**, 17 (1985).

<sup>7</sup>J. A. Appelbaum and D. R. Hamann, Surf. Sci. **74**, 21 (1978).

<sup>8</sup>R. M. Feenstra, J. A. Stroscio, J. Tersoff, and A. P. Fein, Phys. Rev. Lett. **58**, 1192 (1987).

<sup>9</sup>K. C. Pandey, Physica (Amsterdam) **117B & 118B**, 761 (1983).

<sup>10</sup>Th. Berghaus, A. Brodde, H. Neddermeyer, and St. Tosch, Surf. Sci. **184**, 273 (1987).

<sup>11</sup>J. M. Gibson, M. L. McDonald, and F. C. Unterwald, Phys. Rev. Lett. **55**, 1765 (1985).

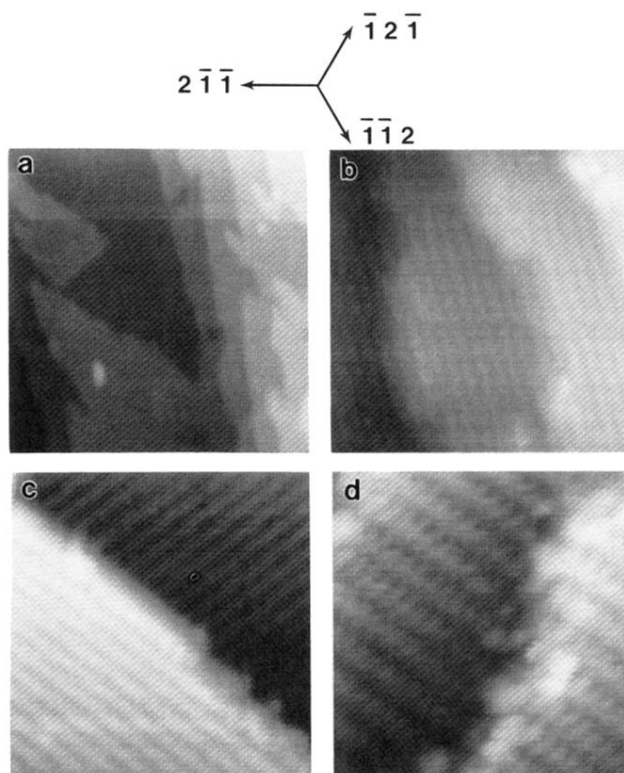


FIG. 1. Large-scale STM images of silicon (111) surfaces, showing atomic steps and the  $2 \times 1$  reconstruction. The images extend over lateral areas of (a)  $600 \times 600 \text{ \AA}^2$ ; (b), (c)  $120 \times 120 \text{ \AA}^2$ ; and (d)  $60 \times 60 \text{ \AA}^2$ .

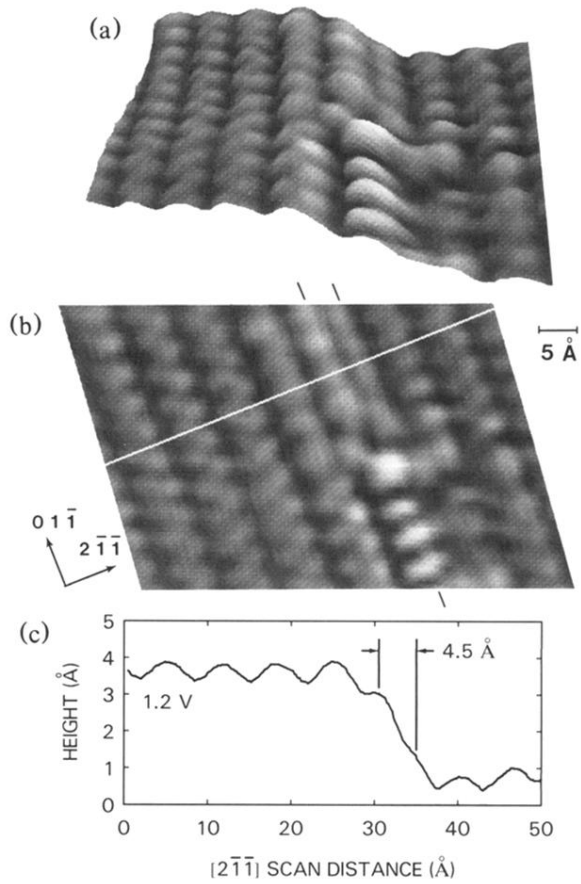


FIG. 2. STM image of a step on Si(111), acquired at sample voltage of +1.2 V; (a) perspective view, (b) top view of the same data, and (c) cross-sectional cut along the line indicated in (b). The step edge is identified by tic marks at the border of the image in (b).

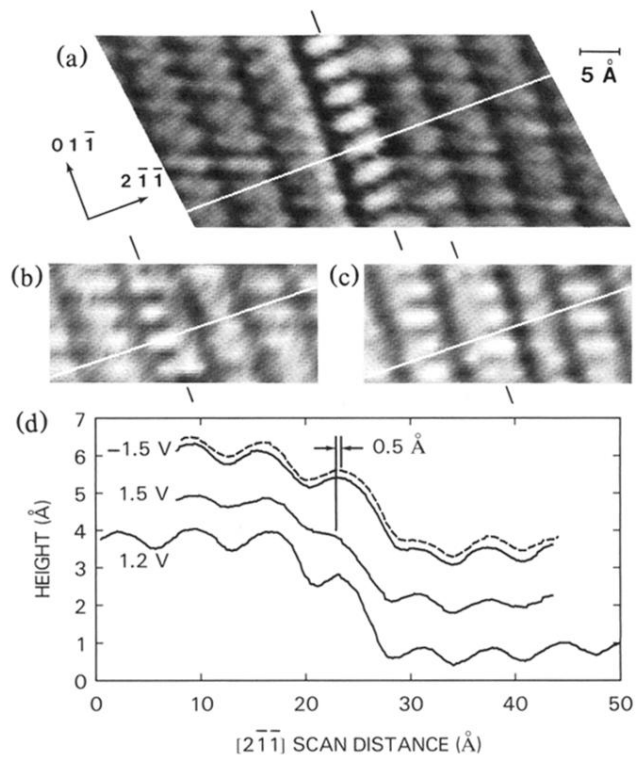


FIG. 3. STM images at various sample voltages; (a) +1.2 V, (b) +1.5 V, and (c)  $-1.5 \text{ V}$ . Images in (b) and (c) were acquired simultaneously. The step edge is identified by tick marks at the border of the images. Cross-sectional cuts of the data are shown in (d); solid lines are cuts taken along the lines indicated in (a)–(c), and the dashed line is a cut taken half a unit cell above the line shown in (c).